Journal of Ceramic Processing Research. Vol. 9, No. 6, pp. 657~660 (2008)

JOURNAL OF
Ceramic Processing Research

Effects of α-Si_3N_4 seeds and sintering additives on properties of porous silicon nitride ceramics fabricated by carbothermal reduction

Yuan Lu, Jian-feng Yang* and Ji-Qiang Gao
State Key Laboratory for Mechanical Behavior of Materials, Xi'an Jiaotong University, Xi'an, Shaanxi 710049, China

In this paper, porous Si_3N_4 ceramics were fabricated by carbothermal reduction between silicon dioxide and carbon [1]. The influences of α-Si_3N_4 seeds and sintering additives on the microstructure and mechanical properties of porous Si_3N_4 ceremics were investigated. XRD analysis proved the complete formation of a single-phase β-Si_3N_4. SEM analysis showed that the resultant porous Si_3N_4 ceramics had a fine microstructure and a uniform pore structure. The sintered sample with Lu_2O_3 as sintering additive showed finer, higher aspect ratio β-Si_3N_4 grains. The addition of Eu_2O_3 accelerated the densification of porous Si_3N_4 ceramics, decreased the porosity and increased the flexural strength. The addition of α-Si_3N_4 seeds accelerated the formation of the α-Si_3N_4 phase at a low temperature and the α-β phase transformation process at a high temperature. With an increase in the α-Si_3N_4 seeds content, the porosity decreased, and the flexural strength increased accordingly.

Key words: Porous silicon nitride ceramics, Carbothermal reduction, Sintering additives, α-Si_3N_4 seeds.

Introduction

Porous Si_3N_4 ceramics with the microstructure of rod-like β-Si_3N_4 grains have better mechanical properties, such as high strength, good thermal shock resistance, high strain and damage tolerance, making them promising candidates for many applications [2].

In this paper, we report on the fabrication of porous Si_3N_4 ceramics by the carbothermal reduction of SiO_2 under a nitrogen atmosphere($3SiO_2 + 6C + 2N_2 \rightarrow Si_3N_4 + 6CO$). We have used silicon dioxide, carbon, a small amount of sintering additives and α-Si_3N_4 seeds as the starting powder [3]. The sintering additives were Y_2O_3, Lu_2O_3 and Eu_2O_3. The effects of different sintering additives and content of α-Si_3N_4 seeds on the microstructure and mechanical properties of porous Si_3N_4 ceramics were investigated. The addition of the sintering additives, which are usually metal oxides that formed a low-melting-point eutectic liquid with the oxide surface layer of the silicon nitride powder, promoted the sintering and densification of silicon nitride ceramics by the liquid sintering mechanism [4]. The addition of α-Si_3N_4 seeds increased the number of α-Si_3N_4 nucleation locations and the rate of nucleation. More α-Si_3N_4 phase was formed consequently at a low temperature. The formation of β-Si_3N_4 at a high temperature was close to the solution-reprecipitation of α-Si_3N_4 in the liquid phase. The addition of a large number of α-Si_3N_4 seeds promoted the nucleation and growth of β-Si_3N_4.

*Corresponding author:
Tel : +86 29 82667942
Fax: +86 29 82665443
E-mail: yang155@mail.xjtu.edu.cn

Experimental Procedure

Quartz SiO_2 (1.8 μm) was used as the starting powder, Y_2O_3, Lu_2O_3 and Eu_2O_3 were used as sintering additives. Carbon black powder (80 nm) and α-Si_3N_4 powder (0.5 μm) were used as the carbon source and seeds respectively. The compositions of the starting powder mixture contain a stoichiometric ratio of C and SiO_2 (2 : 1 molar ratio), corresponding to 5 wt% sintering additive and different contents of α-Si_3N_4 seeds. The powder mixture was ball-milled with high-purity silicon nitride balls in anhydrous alcohol for 24 h in a plastic bottle. After milling, the slurry was dried by a rotary evaporator and sieved through a 150 μm screen. The mixed powders were then uniaxially pressed to form rectangular bars measuring 46 mm × 5 mm × 5 mm. The green bodies were sintered in a furnace (High multi-5000 Fijidempa Co. ltd., Osaka, Japan) at 1750_o for 2 h.

The bulk density of the sintered products was measured by the Archimedes displacement method. Crystalline phases were identified by XRD (D/MAX-2400X, Rigaku Co., Tykyo, Japan) analysis. The microstructure was characterized by SEM (JSM-35C, JEOL, Japan). The three-point bending strength was measured on specimen bars with a span of 16 mm at a cross-head speed of 0.5 mm/minute by an instrument (Instron 1195, Instron Co., England). Each final value was averaged over five measurements. The sample designations and their compositions in this paper are shown in Table 1.

Results and Discussions

Variations in the weight loss, shrinkage, porosity, flexural

Table 1. Composition of the samples

Samples	Composition
Lu 5%	64.3 wt% SiO_2 + 25.7 wt% C + 5 wt% Lu_2O_3 + 5 wt% α-Si_3N_4 seeds
Eu 5%	64.3 wt% SiO_2 + 25.7 wt% C + 5 wt% Eu_2O_3 + 5wt% α-Si_3N_4 seeds
Y 5%	64.3 wt% SiO_2 + 25.7 wt% C + 5 wt% Y_2O_3 + 5 wt% α-Si_3N_4 seeds
Y20%	53.6 wt% SiO_2 + 21.4 wt% C + 5 wt% Y_2O_3 + 20 wt% α-Si_3N_4 seeds
Y50%	32.1 wt% SiO_2 + 12.9 wt% C + 5 wt% Y_2O_3 + 50 wt% α-Si_3N_4 seeds

Table 2. Summary of sintering behavior and mechanical properties of porous Si_3N_4 ceramics

Samples	Weight loss [%]	Linear shrinkage [%]	Porosity [%]	Flexural strength [MPa]
Lu 5%	45	3.40	78	2.3
Eu 5%	45	17.5	60	34
Y 5%	48	15.2	79	3.5
Y20%	44	11.8	73	12.5
Y50%	29	6.1	68	37.7

strength with different sintering additives and content of α-Si_3N_4 seeds are shown in Table 2. The porosity of the porous Si_3N_4 ceramics after the carbothermal reduction was mainly affected by the linear shrinkage and the weight loss during the reaction. The linear shrinkage and weight loss were two main factors determining the porosity of the sintered samples. As shown in Table 2, there was no obvious difference in the weight loss for the samples with different sintering additives and the theoretical weight loss after the complete carbothermal reduction was about 44%. The weight loss in the sintered samples was mainly the result of the loss of carbon black in the carbothermal reduction. The linear shrinkage resulted from a very large amount of weight loss and the sintering driving force at a high temperature. The samples Y 5% and Lu 5% showed lower linear shrinkage which caused higher porosities. So the samples Y 5% and Lu 5% exhibited a poor sinterability by comparison with the sample Eu 5% which exhibited an excellent sinterability. This was because the sample Eu 5% is superior to samples Y 5% and Lu 5% in promoting densification of silicon nitride by lowering the eutectic temperature and viscosity of the liquid phase. Because there was a large difference in the linear shrinkage for the different samples, there was also a large difference in the porosity for the samples with different sintering additives.

For the samples with different contents of α-Si_3N_4 seeds, there was an obvious difference in the weight loss and the linear shrinkage. With an increase in the content of α-Si_3N_4 seeds, the weight loss, the linear shrinkage and the porosity decreased, Because the theoretical weight loss after the complete carbothermal reduction was about 44%, which was mainly the result of the loss in the carbothermal reduction, so with an increase in the content of α-Si_3N_4 seeds, the content of carbon black decreased accordingly. So the weight loss after the complete carbothermal reduction decreased. Although the linear shrinkage of the samples decreased accordingly, the influence of the weight loss on the porosity of samples was much more extensive than the influence of the linear shrinkage on it. So with an increase in the content of α-Si_3N_4 seeds, the porosity of samples decreased.

The XRD analyses for the samples with different contents of α-Si_3N_4 seeds and sintering additives is shown in Fig. 1. Only β-Si_3N_4 phase was detected by XRD analysis. No α-Si_3N_4 phase was detected in the diffraction patterns, confirming a full transformation from α-Si_3N_4 to β-Si_3N_4 during the high-temperature sintering. No grain boundary phase was detected. The explanation is that any grain boundary phase present was in such small quantities that it could not be detected by XRD analysis.

The silicon nitride fabricated by carbothermal reduction transformed from α-Si_3N_4 to β-Si_3N_4 by the solution-precipitation process. No second phase particles were identified in the microstructure, indicating that all the sintering additives were dissolved in the eutectic liquid

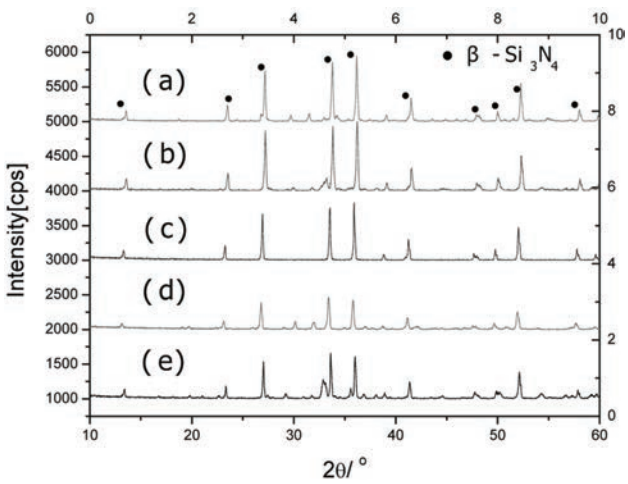

Fig. 1. XRD patterns of the porous silicon nitride ceramics obtained with different sintering additives and content of α-Si_3N_4 seeds (a) Eu 5% (b) Lu 5% (c) Y 5% (d) Y 20% (e) Y 50%.

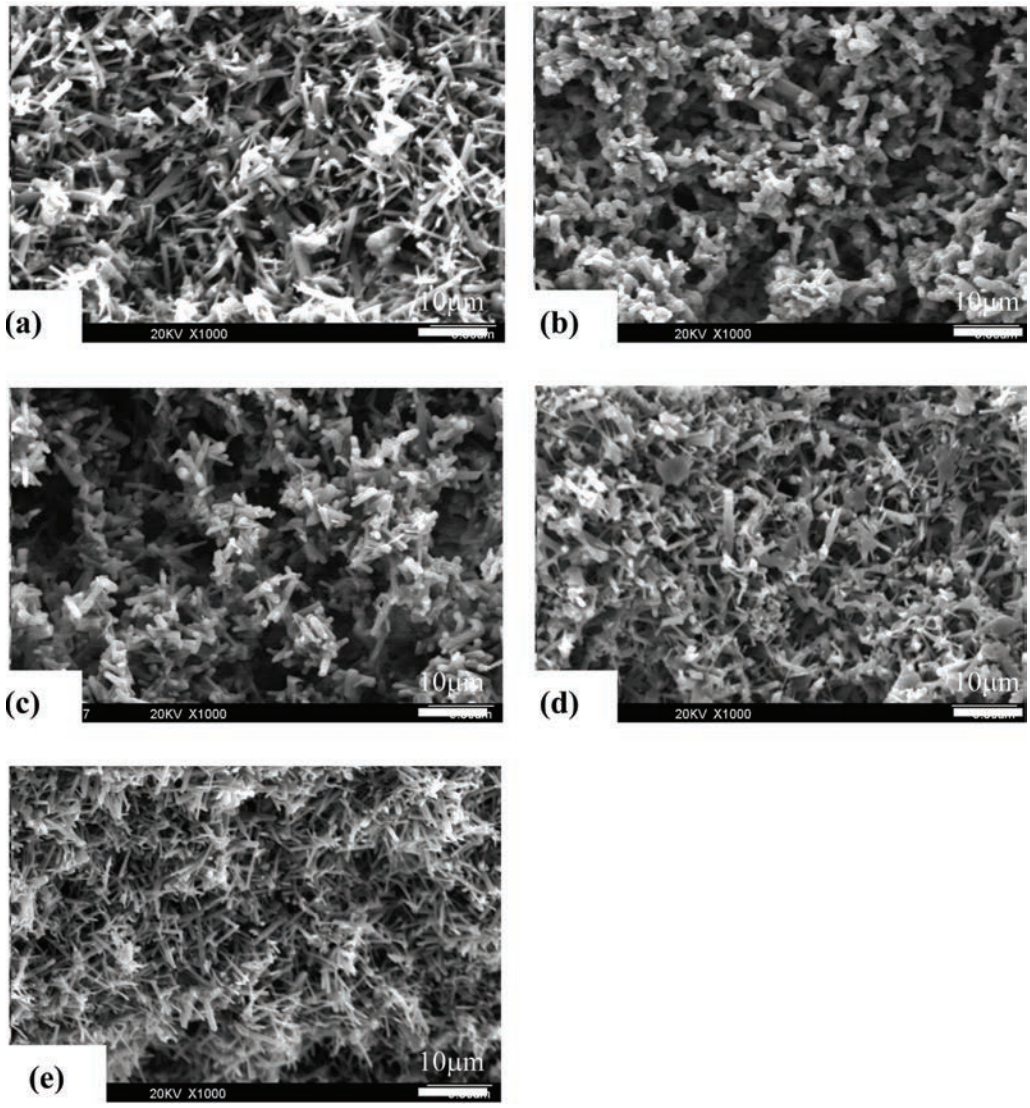

Fig. 2. SEM images of porous silicon nitride ceramics with different sintering additives and contents of α-Si_3N_4 seeds (a) Lu 5% (b) Eu 5% (c) Y 5% (d) Y20% (e) Y50%.

during the sintering process. This was consistent with the former XRD results. Fig. 2 gives SEM images of fracture surfaces of the sintered samples with different sintering additives and content of α-Si_3N_4 seeds. It was obvious that these samples showed a typical microstructure composed of fine elongated β-Si_3N_4 grains with a high aspect ratio and a uniform pore structure. Furthermore, it was observed that there were two obvious differences in the microstrucure for the samples with different sintering additives; 1) a difference in the aspect ratio of the fine elongated β-Si_3N_4 grains with different sintering additives; 2) a difference in the pores size with different sintering additives. Compared with sample Eu 5% , samples Y 5% and Lu 5% showed a higher aspect ratio of the β-Si_3N_4 grains. The explanation was that the sintering additive controlled the aspect ratio of β-Si_3N_4 grains and pore sizes by its effects on the viscosity of the liquid phase. The sintering additives which were used in this article were all rare-earth oxides, rare-earth oxides elements with larger ionic radii produce a higher viscosity of liquid phase. So element Lu with the largest ionic radii showed the highest aspect ratio of the β-Si_3N_4 grains due to the highest viscosity of the liquid phase. By contrast, element Eu with the smallest ionic radii showed the lowest aspect ratio of the β-Si_3N_4 grains due to the lowest viscosity of the liquid phase.

Fig. 2 also gives SEM images of fracture surfaces of the sintered samples with different contents of α-Si_3N_4 seeds. The addition of 5 wt% α-Si_3N_4 seeds increased the number of α-Si_3N_4 nucleation sites. The nucleation and growth of α-Si_3N_4 occurred on the planes of α-Si_3N_4 grains directly. The rate of nucleation was increased. Much of the α-Si_3N_4 phase was formed consequently at a low temperature. The formation of β-Si_3N_4 at a high temperature was close to the solution-reprecipitation of α-Si_3N_4 in the liquid phase. The solution of a large number of α-Si_3N_4 particles promoted the supersaturation of the liquid phase, as well as the nucleation and growth of β-Si_3N_4. So sample Y 5%

showed fine elongated β-Si_3N_4 grains with a higher aspect ratio and a uniform pore structure. Sample Y 20% showed a bimodal microstructure composed of large elongated β-Si_3N_4 grains and finer β-Si_3N_4 grains. But some of the β-Si_3N_4 grains with a large particle size were coarse. Although, the average particle size of β-Si_3N_4 was small, it was not observed that there were fine elongated β-Si_3N_4 grains with a higher aspect ratio and a uniform pore structure in the microstructure. This was because the addition of α-Si_3N_4 seeds was extensive and it decreased the contact area of the reactants (C and SiO_2) which is important in determing the carbothermal reduction. Even if the addition of 20 wt% α-Si_3N_4 seeds increased the number of α-Si_3N_4 nucleation sites, the rate of nucleation was very low, and consequently only a small quantity of α-Si_3N_4 phase was formed at the low temperature. So sample Y 20% exhibited coarse β-Si_3N_4 grains with a lower aspect ratio. Although the addition of 50 wt% α-Si_3N_4 seeds was very disadvantageous to the carbothermal reduction, 50 wt% α-Si_3N_4 accelerated the formation of the α-Si_3N_4 phase at a low temperature and the α-β phase transformation process at a high temperature. So sample Y 50% showed fine elongated β-Si_3N_4 grains with a higher aspect ratio and a uniform pore structure.

The flexural strength of porous Si_3N_4 ceramics depended on their microstructure and porosity. The porous Si_3N_4 ceramics showed a fine microstructure, a high aspect ratio of β-Si_3N_4 grains which contributed to a relatively higher flexural strength. If the flexural strength of porous ceramics is expressed as a function of porosity, the flexural strength decreased exponentially with the porosity. As shown in Table 2, with the lowest porosity, the sample Eu 5% showed the highest flexural strength. Compared with the sample Eu 5%, the sample Lu 5% showed a better microstructure with a higher aspect ratio β-Si_3N_4 grains. But the porosity of the sample Eu 5% was much less than the porosity of the sample Lu 5%. So the sample Eu 5% showed the highest flexural strength.

With an increase in the content of α-Si_3N_4 seeds, the porosity decreased accordingly. The flexural strength decreased exponentially with the porosity. So with an increase in the content of α-Si_3N_4 seeds, the flexural strength increased accordingly. Sample Y 5% and sample Y 50% which showed fine elongated β-Si_3N_4 grains with a higher aspect ratio and a uniform pore structure have relatively higher flexural strengths. But the porosity in the sample Y 20% was much less than the porosity in the sample Y 5%. So the sample Y 20% showed the higher flexural strength.

Summary

The sample with Lu_2O_3 as a sintering additive showed higher aspect ratio β-Si_3N_4 grains. The sample with Eu_2O_3 as a sintering additive exhibited the highest flexural strength due to having the lowest porosity. The addition of α-Si_3N_4 seeds accelerated the formation of the α-Si_3N_4 phase at a low temperature and the α-β phase transformation process at a high temperature. With an increase in the content of α-Si_3N_4 seeds, the porosity decreased and the flexural strength increased accordingly.

Acknowledgements

The authors wish to express thanks for the financial support of the State Education Ministry of the People's Republic of China (RFDP Program (20060698008), SRF for ROCS Program (05-04) and NCET Program (04-0941)), and Science and Technology Department of Shannxi Province (Project No. 2004K07-G13).

References

1. S.Y. Shan, J.F. Yang and J.Q. Gao, J. Am. Ceram. Soc. 88 (2005) 2594-2596.
2. S.Y. Shan, J.F. Yang and Y. Lu, Scr. Mater. 56 (2007) 193-196.
3. J.F. Yang and S.Y. Shan, Acta Mater. 53 (2005) 2981-2990.
4. J. Yang, J.F. Yang and S.Y. Shan, J. Am. Ceram. Soc. 89 (2006) 3843-3845.